Gold Nanoparticle-Based Core−Shell and Hollow Spheres and Ordered Assemblies Thereof

Zhijian Liang,[†] Andrei Susha,[†] and Frank Caruso*[,‡]

Max Planck Institute of Colloids and Interfaces, D-14424 Potsdam, Germany, and Department of Chemical and Biomolecular Engineering, The University of Melbourne, Victoria 3010, Australia

Received January 13, 2003. Revised Manuscript Received May 22, 2003

We report on the preparation and characterization of gold nanoparticle (Au_{NP})-based core−shell particles and hollow spheres and of ordered structures obtained from their self-assembly. Coated particles, comprising polystyrene (PS) cores and polyelectrolyte (PE) or Au_{NP}/PE shells, were prepared by the layer-by-layer technique, that is, via the sequential adsorption of oppositely charged PEs onto PS cores, or by the infiltration of gold nanoparticles into preassembled PE multilayers onto PS particles, respectively. The thickness of the gold nanoparticle-based coatings was varied by altering the number of preassembled PE layers into which gold nanoparticles were infiltrated and by additional electroless gold plating. Hollow spheres were obtained from the core−shell particles by either calcination or by dissolution of the PS core by exposure to tetrahydrofuran. The coated colloids were used as building blocks for the construction of ordered particle assemblies. Two different approaches were employed to form the ordered particle structures. The first involved the gravity sedimentation of Au_{NP}/PE-coated PS spheres, while the second method entailed the formation of ordered assemblies of PE-coated PS spheres, followed by infiltration with gold nanoparticles. 3D macroporous ("hollow") ordered structures were subsequently prepared from the ordered core−shell particle assemblies by removal of the PS cores. UV−visible absorption measurements of core−shell and hollow Au_{NP}/PE microspheres, and 3D ordered assemblies of these particles, show red-shifted plasmon resonance bands relative to the gold nanoparticles in solution. Near-IR reflectance spectra of the 3D ordered structures of hollow Au_{NP}/PE microspheres show Bragg reflectance peaks that are blue-shifted relative to the corresponding structures prior to dissolution of the core. The strategy described opens a new avenue to the production of particle assemblies derived from core−shell and hollow colloids, which may provide new opportunities for their application in areas such as photonics, photoelectronics, and catalysis.

Introduction

The organization of metal nanoparticles into diverse structures is essential for their application in optical, electronic, and magnetic devices.[1] Metal nanoparticles have been assembled into monolayer or multilayer thin films on planar surfaces,[1−3] 2D or 3D superlattices,[4−8] nanowires,[9−15] macroporous structures,[16] and colloidal aggregates.[17−20] Recently, metal nanoparticles have also found use as building blocks to construct core−shell particles[21−32] and hollow spheres.[21,32−34] The properties

* To whom correspondence should be addressed. Fax: +61 3 8344 4153. E-mail: fcaruso@unimelb.edu.au.
[†] Max Planck Institute of Colloids and Interfaces.
[‡] The University of Melbourne.

(1) Shipway, A. N.; Kaltz, E.; Willner, I. *ChemPhysChem*. **2000**, *1*, 18.
(2) Musick, M. D.; Keating, C. D.; Natan, M. J. *Chem. Mater*. **1997**, *9*, 1499.
(3) Gittins, D. I.; Bethell, D.; Nichols, R. J.; Schiiffrin, D. J. *Adv. Mater*. **1999**, *11*, 737.
(4) Whetten, R. L.; Shafigullin, M. N.; Khoury, J. T.; Schaaf, T. G.; Vezmar, I.; Alvarez, M. M.; Wilkinson, A. *Acc. Chem. Res.* **1999**, *32*, 397.
(5) Collier, C. P.; Vossmeyer, T.; Heath, J. R. *Annu. Rev. Phys. Chem*. **1998**, *49*, 371.
(6) Taleb, A.; Petit, C.; Pileni, M. P. *J. Phys. Chem. B* **1998**, *102*, 2214.
(7) Wang, Z. L. *Adv. Mater*. **1998**, *10*, 13.
(8) Kiely, C. J.; Fink, J.; Brust, M.; Bethell, D.; Schiffrin, D. J. *Nature* **1998**, *396*, 444.
(9) Marinakos, S. M.; Brousseau, L. C.; Jones, A.; Feldheim, D. L. *Chem. Mater*. **1998**, *10*, 1214.
(10) Zhou, Y.; Yu, S. H.; Cui, X. P.; Wang, C. Y.; Chen, Z. Y. *Chem. Mater*. **1999**, *11*, 545.
(11) Korgel, B. A.; Fitzemaurice, D. *Adv. Mater*. **1998**, *10*, 661.
(12) Simon, U.; Schon, G.; Schmid, G. *Angew. Chem., Int. Ed. Engl*. **1993**, *32*, 250.
(13) Kumar, A.; Pattarkine, M.; Bhadhade, M.; Mandale, A. B.; Ganesh, K. N.; Datar, S. S.; Dharmadhikari, C. V.; Sastry. M. *Adv. Mater*. **2001**, *13*, 341.
(14) Hermanson, K. D.; Lumsdon, S. O.; Williams, J. P.; Kaler, E. W.; Velev, O. D. *Science* **2001**, *294*, 1082.
(15) Sun, Y.; Gates, B.; Mayers, B.; Xia, X. *Nano Lett*. **2002**, *2*, 165.
(16) (a) Velev, O. D.; Tessier, P. M.; Lenhoff, A. M.; Kaler, E. W. *Nature* **1999**, *401*, 548. (b) Jiang, P.; Cizeron, J.; Bertone, J. F.; Colvin, V. L. J. *Am. Chem. Soc*. **1999**, *121*, 7957.
(17) Mirkin, C. A.; Letsinger, R. L.; Music, R. C.; Storhoff, J. J. *Nature* **1996**, *382*, 607.
(18) Shenton, W.; Davis, S. A.; Mann, S. *Adv. Mater*. **1999**, *11*, 449.
(19) Boal, A. K.; Llhan, F.; Derouchy, J. E.; Thurn-Albrecht, T.; Russell, T. P.; Rotello, V. M. *Nature* **2000**, *404*, 746.
(20) Maye, M. M.; Chun, S. C.; Han, L.; Rabinovich, D.; Zhong, C. J. *J. Am. Chem. Soc*. **2002**, *124*, 4958.
(21) Graf, C.; van Blaaderen, A. *Langmuir* **2002,** *18,* 524.

10.1021/cm031014h CCC: $25.00
Published on Web 07/09/2003

of these particles can be distinctly different from those of individual nanoparticles. For example, they can possess unique size-dependent optical, electronic, and catalytic properties, thereby making them of promise in technological applications such as photonic materials, surface-enhanced Raman scattering, chemical and biological sensing, and catalysis.[21−34]

One approach at the forefront of the preparation of coated and hollow spheres is the layer-by-layer (LbL) assembly method.[35] By sequentially adsorbing oppositely charged species onto colloid templates, a variety of core−shell and hollow particles of various composition (from organic to inorganic and composites) can be prepared.[35] Metal nanoparticles such as gold, Au@SiO_2,[32] and octa(3-aminopropyl)silsesquioxane (NSi8) stabilized Ag[26] have been used as components for the construction of such composite and hollow spherical particles. For the preparation of hollow spheres from precursor core−shell particles comprising nanoparticle shells through calcination, a close packing of the coating nanoparticles is required.[26,32,35a−f] When gold nanoparticles are used, the surface coverage is typically around 30%.[24] This surface coverage can be increased to be close to that of a close-packed monolayer if surface-modified metal nanoparticles are used.[26,32] For example, the presence of a thin silica[32] or NSi8[26] coating on the nanoparticles can be exploited to allow them to pack closely together. However, such surface coatings can prevent the subsequent metallization of the deposited nanoparticles (or coatings) through, for example, electroless plating. The ability to control the morphology and structure of the coatings (e.g., nanoparticulate, continuous, etc.) through electroless plating is particularly of interest in applications that require tailored optical properties.[22]

Recently, in an alternative strategy, we reported that significantly increased surface coverages (up to monolayer coverage, which corresponds to ∼74%, and even higher) can be obtained by exploiting the adsorption behavior of gold nanoparticles stabilized by 4-(dimethylamino)pyridine (DMAP) (Au_{NP}) into preassembled polyelectrolyte (PE) multilayers on colloid particles.[31] We also showed that these Au_{NP}/PE-coated particles can be assembled into ordered arrays, which display tunable optical properties depending on the gold nanoparticle loading.[36] In this paper, we present a detailed study on the preparation and characterization of core−shell and hollow spheres based on DMAP-stabilized gold nanoparticles. Additionally, ordered assemblies of the core−shell particles formed through gravity sedimentation and water evaporation were used as templates to prepare ordered assemblies of hollow Au_{NP}/PE microspheres. The optical properties of the dispersions of core−shell and hollow spheres and the ordered assemblies were investigated by UV−visible absorption and near-IR reflection spectroscopy.

Experimental Section

Materials. Poly(allylamine hydrochloride) (PAH), M_w 70000, poly (sodium 4-styrene sulfonate) (PSS), M_w 70000, poly(ethylenimine) (PEI), M_w 25000, poly(diallyldimethylammonium chloride) (PDADMAC), M_w < 200000, chloroauric acid ($HAuCl_4$), and hydroxylamine hydrochloride ($NH_2OH{\cdot}HCl$) were obtained from Sigma-Aldrich and used as received, except for PSS, which was dialyzed against Milli-Q water (M_w cutoff 14 kDa) and lyophilized before use. Jeffamine M2070, a random copolymer of 70% PEO with 30% poly(propylene oxide), M_w 2000, was obtained from Huntsman Chemicals. The negatively charged sulfate-stabilized polystyrene (PS) particles, diameter 640 nm, were prepared as described elsewhere.[37] The 4-(dimethylamino)pyridine (DMAP)-stabilized gold nanoparticles (6 ± 2 nm diameter, positively charged), Au_{NP}, were prepared as described previously.[38] The water used in all experiments was prepared in a three-stage Millipore Milli-Q Plus 185 purification system and had a resistivity higher than 18.2 MΩ·cm.

Preparation of the Core−Shell Particles. Before adsorption of the Au_{NP}, the PS spheres were coated with PE multilayers:[36] 0.5 mL of positively charged PAH or PDADMAC (1 mg mL^{-1} in water containing 0.5 M NaCl) was added to 0.5 mL of a dispersion of negatively charged (1 wt %) 640-nm-diameter PS spheres. After 15 min, the excess polyelectrolyte was removed by three centrifugation (6800*g*, 10 min)/washing cycles. Next, negatively charged polyelectrolyte (PSS) was deposited using the same conditions and procedure. The above process was repeated until the desired number of PE layers (2−8) was deposited. In some cases a layer of the amine-terminated PEO copolymer was adsorbed onto the spheres (with an outermost PSS layer) at pH 3 for 15 min, followed by removal of the excess copolymer by three centrifugation (6800*g*, 10 min)/washing cycles. The PE_x/Au_{NP}-coated PS spheres were prepared by adding 1 mL of a 0.5 wt % dispersion of the PE_x-coated PS particles (with $x = 2$, 4, 6, or 8; outermost layer = PSS) to a 10-mL dispersion of the positively charged DMAP-stabilized Au_{NP} (concentration of ca. 1×10^{15} particles mL^{-1}).[31,36] An adsorption time of 24 h was used to ensure Au_{NP} adsorption. The coated PS particles were then subjected to three centrifugation (960*g*, 10 min)/washing cycles and additionally coated with two PE layers (PEI and PSS) to prevent possible aggregation of the composite colloid particles formed.

(22) (a) Oldenburg, S. J.; Averitt, R. D.; Westcott, S. L.; Halas, N. J. *Chem. Phys. Lett.* **1998**, *288*, 243. (b) Westcott, S. L.; Oldenburg, S. J.; Randall Lee, T.; Halas, N. J. *Langmuir* **1998**, *14*, 5396.
(23) Ji, T.; Lirtsman, V. G.; Avny, Y.; Davidov, D. *Adv. Mater.* **2001**, *13*, 1254.
(24) Dokoutchaev, A.; James, J. T.; Koene, S. C.; Pathak, S.; Prakash, G. K. S.; Thompson, M. E. *Chem. Mater.* **1999**, *11*, 2389.
(25) (a) Chen, C. W.; Chen, M. Q.; Serizawa, T.; Akashi, M. *Chem. Commun.* **1998**, 831. (b) Chen, C. W.; Serizawa, T.; Akashi, M. *Chem. Mater.* **1999**, *11*, 1381. (c) Chen, C. W.; Chen, M. Q.; Serizawa, T.; Akashi, M. *Adv. Mater.* **1998**, *10*, 122.
(26) (a) Cassagneau, T.; Caruso, F. *Adv. Mater.* **2002**, *14*, 732. (b) Cassagneau, T.; Caruso, F. *J. Am. Chem. Soc.* **2002**, *124*, 8172.
(27) Kobayashi, Y.; Salgueirino-Maceira, V.; Liz-Marzan, L. M *Chem. Mater.* **2001**, *13*, 1630.
(28) (a) Zhong, Z.; Mastai, Y.; Koltypin, Y.; Zhao, Y.; Gedanken, A. *Chem. Mater.* **1999**, *11*, 2350. (b) Ramesh, S.; Cohen, Y.; Prosorov, R.; Shafi, K. V. P. M.; Aurbach, D.; Gedanken, A. *J. Phys. Chem. B* **1998**, *102*, 10234.
(29) Warshawsky, A.; Upson, D. A. *J. Polym. Sci., Part A*: *Polym. Chem.* **1989**, *27*, 2963.
(30) Mayer, A. B. R.; Grebner, W.; Wannemacher, W. *J. Phys. Chem. B* **2000**, *104*, 7278.
(31) Gittins, D. I.; Susha, A. S.; Schoeler, B.; Caruso, F. *Adv. Mater.* **2002**, *14*, 508.
(32) Caruso, F.; Spasova, M.; Salgaueirino-Maceira, V.; Liz-Marzan, L. M. *Adv. Mater.* **2001**, *13*, 1090.
(33) Kim, S.; Kim, M.; Lee, W.; Hyeon, T. *J. Am. Chem. Soc.* **2002**, 124, 7642.
(34) Wong, M. S.; Cha, J. N.; Choi, K.; Deming, T. J.; Stucky, G. D. *Nano Lett.* **2002**, *2*, 583.
(35) (a) Caruso, F.; Caruso, R. A.; Möhwald, H. *Science* **1998**, *282*, 1111. (b) Donath, E.; Sukhorukov, G. B.; Caruso, F.; Davis, S. A.; Möhwald, H. *Angew. Chem., Int. Ed.* **1998**, *37*, 2201. (c) Caruso, F. *Adv. Mater.* **2001**, *13*, 11. (d) Caruso, F. *Chem. Eur. J.* **2000**, *6*, 413. (e) Caruso, F.; Spasova, M.; Susha, A.; Giersig, M.; Caruso, R. A. *Chem. Mater.* **2001**, *13*, 109. (f) Caruso, R. A.; Susha, A.; Caruso, F. *Chem. Mater.* **2001**, *13*, 400.
(36) Liang, Z.; Susha, A. S.; Caruso, F. *Adv. Mater.* **2002**, 14, 1160.
(37) Furusawa, K.; Norder, W.; Lyklema, J. *Kolloid-Z. Z. Polym.* **1972**, *250*, 908.
(38) Gittins, D. I.; Caruso, F. *Angew. Chem., Int. Ed.* **2001**, *40*, 3001.

Electroless Plating of Au_{NP}-Coated Particles. The adsorbed Au_{NP} can serve as seeds for subsequent shell growth by electroless gold plating.[21−23] Two hundred microliters of a 0.8 wt % Au_{NP}/PE-coated PS dispersion was diluted to 20 mL with water, and then a mixture of 0.1−0.5 mL of 1 wt % $HAuCl_4$ and 0.5−2.5 mL of 0.04 M $NH_2OH{\cdot}HCl$ was added under stirring for 10 min. For electroless plating of the PS−$(PAH/PSS)_2/Au_{NP}$/PEI/PSS and $(PDADMAC/PSS)_2/Au_{NP}$/PEI/PSS particles, 0.1 mL of 1 wt % $HAuCl_4$ and 0.5 mL of 0.04 M $NH_2OH{\cdot}HCl$, and 0.3 mL of 1 wt % $HAuCl_4$ and 1.5 mL of 0.04 M $NH_2OH{\cdot}HCl$, were used, respectively. The plated particles were then coated with two additional layers of polyelectrolyte (PEI and PSS).

Crystallization of the Core−Shell Particles. The cell employed for crystallization consists of a Teflon ring of 1-cm inner diameter, a quartz slide (which was cleaned according to the RCA protocol[39]), and two fixed steel plates to prevent leakage of the liquid.[36] One hundred microliters of the particle dispersions of about 1 wt % were added into the chamber over the accessible quartz area encircled by the Teflon ring. Samples were kept at room temperature, and the coated colloids were crystallized by gravity sedimentation and water evaporation.

Nanoparticle Infiltration of Colloidal Crystals and Electroless Gold Plating. To infiltrate the ordered assemblies of PE_x/PEO-coated PS spheres with the gold nanoparticles, the samples were immersed in the Au_{NP} solution for 24 h and then washed with water (3 × 10 s). The gold nanoparticles that infiltrated into the colloidal crystals were used as seeds for subsequent shell growth by electroless gold plating. This was achieved by sequentially dipping the quartz substrate with the ordered assemblies of PE/PEO-coated PS colloidal crystals infiltrated with gold nanoparticles into a 2 wt % $HAuCl_4$ solution for 2 h, and then into a 0.4 M $NH_2OH{\cdot}HCl$ solution for 1 h. Higher gold coverages were obtained by repeating the $HAuCl_4$ and $NH_2OH{\cdot}HCl$ stages.

Hollow Spheres and Ordered Assemblies. Both nonplated and gold-plated core−shell particles and their ordered assemblies were used to produce hollow gold spheres and ordered assemblies thereof by either calcination (at 310 °C for 2 h in N_2 and then at 310 °C for 22 h in O_2), causing removal of the core and polyelectrolyte, or by dissolution of the PS core by tetrahydrofuran (THF) treatment (for 0.5 h in the case of separated particles in solution or for 12 h in the case of quartz-supported ordered arrays). After THF treatment, the samples were subsequently washed with THF and water.

Characterization Methods. Transmission electron microscopy (TEM) measurements were performed with a Philips CM12 microscope operated at 120 kV. Scanning electron microscopy (SEM) images were recorded with a JEOL (JSEM 6330 F) instrument operated at an acceleration voltage of 5 kV. For SEM investigations, 5 nm of Pd or Au film was sputter-coated onto the samples prior to measurement. The UV−visible absorption data were recorded on a Cary 4E spectrophotometer. The reflectance spectra were collected on a Cary 500 spectrophotometer and were taken at an angle of incidence of 20° to the (111) crystal plane. A Netzsch TG 209 apparatus was used for thermogravimetric analysis of the coated particles, which were heated between 20 and 700 °C in oxygen. The weight percent of gold was determined as the ratio of the mass of the samples after heating to 700 °C, which leads to the oxidation of all organic materials, to the initial mass of the samples.

Results and Discussion

A. Core−Shell Particles and Hollow Spheres. *(a) Preparation and Characterization.* Before gold nanoparticle adsorption, PS spheres of 640-nm diameter were coated with 2−8 multilayers of PAH and PSS or PDADMAC and PSS by the LbL approach.[35] The outermost layer was negative to promote adsorption of the positively charged Au_{NP}. The 4-(dimethylamino)-pyridine (DMAP)-stabilized gold nanoparticles (6 ± 2 nm diameter) were prepared by synthesis in toluene, followed by phase transfer to water.[38] Au_{NP}/PE-coated PS spheres were prepared by exposing the PAH/PSS or PDADMAC/PSS multilayer-coated PS spheres (with different coating thickness) to a Au_{NP} dispersion in water. This resulted in the nanoparticles infiltrating and binding to the PE layers,[31] giving a dense and uniform Au_{NP} coating (Figure 1a,b). The thickness of the Au_{NP} layer was varied by changing the number of preassembled PE layers. Figure 1a,b shows TEM images of PS spheres coated with 4 and 8 PE layers, respectively, and subsequently exposed to a Au_{NP} dispersion. The diameters of the coated spheres are 678 ± 5 and 694 ± 5 nm, respectively, corresponding to an average diameter increase of 38 ± 5 and 54 ± 5 nm (relative to pure 640-nm PS). TEM and single-particle light-scattering measurements on PAH/PSS-coated particles indicate a thickness increment of 1.5 nm/PE layer[35] (shell thickness of about 6 and 12 nm for the PE_4- and PE_8-coated PS spheres, respectively), giving a diameter increase of 26 ± 5 and 30 ± 5 nm due to adsorption of the gold nanoparticles. Thermogravimetric analysis (TGA) indicated that the gold content in the samples increases with increasing PE layer thickness. For the PS−PE_x/Au_{NP}/PEI/PSS particles, the gold content was 47, 57, and 59 wt % for $x = 4$, 6, and 8, respectively.[36] It is noted that to increase the colloidal stability of the composite particles formed, an additional two-layer PE coating (PEI/PSS) was deposited.

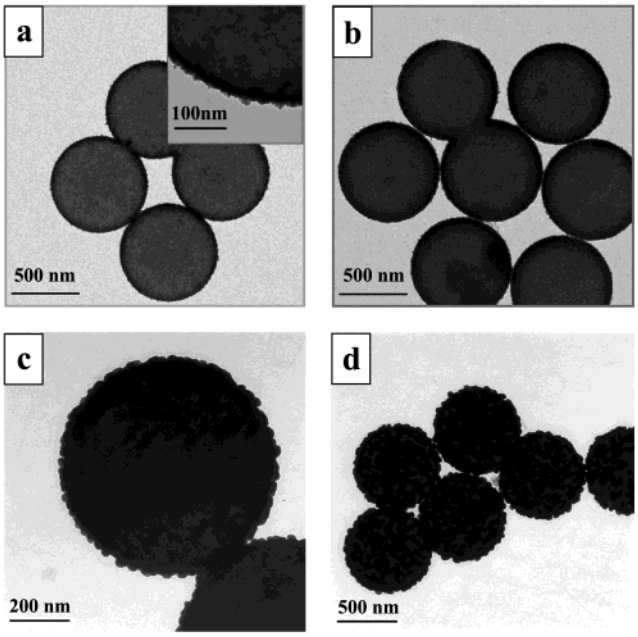

Figure 1. TEM images of PS−$(PAH/PSS)_x/Au_{NP}$ spheres with $x = 2$ (a) and $x = 4$ (b), PS−$(PAH/PSS)_2/Au_{NP}$/(PEI/PSS) spheres after electroless gold plating (c), and PS−$(PDADMAC/PSS)_2/Au_{NP}$/(PEI/PSS) after electroless gold plating (d). The PEI/PSS layers were deposited after electroless plating (c and d).

Gold nanoparticles deposited on the surface of the PS spheres can serve as seeds for subsequent shell growth by electroless plating.[22] Such treatment results in a

(39) Riegler, H.; Engel, M. *Ber. Bunsen-Ges. Phys. Chem.* **1991**, *95*, 1424.

uniform increase in gold coverage, and in turn an increase in the particle diameter (Figure 1c,d). For PS−$(PAH/PSS)_2/Au_{NP}$/PEI/PSS and PS−$(PDADMAC/PSS)_2/Au_{NP}$/PEI/PSS particles, electroless plating (see Experimental Section) results in an increase in the particle diameters to 734 ± 5 and 745 ± 5 nm, respectively. The increase in particle diameter as a result of plating is 50 ± 5 nm for the PS−$(PAH/PSS)_2/Au_{NP}$/PEI/PSS particles and 79 ± 5 nm for the PS−$(PDADMAC/PSS)_2/Au_{NP}$/PEI/PSS particles. The larger increase for the latter particles is due to the use of more $HAuCl_4$ (0.3 mL vs 0.1 mL of 1 wt % $HAuCl_4$) for their plating. It was possible to continue to increase the particle diameter with electroless plating, but we found that such particles have lower colloidal stability and aggregate easily.

In our earlier studies on PS particles coated with PE multilayers and nanoparticles (e.g., SiO_2, TiO_2, Fe_3O_4, Au@SiO_2, octa(3-aminopropyl)silsesquioxane-stabilized Ag), we showed that hollow spheres could be formed by either thermal or chemical means.[26,32,35] In the first approach, pure inorganic hollow spheres were formed, as calcination removes both the PS core and bridging PEs. In the second route, the hollow spheres consist of PE and inorganic nanoparticles. In the current work, both thermal and chemical approaches were investigated. It was found that despite the high melting temperature of bulk gold (∼1064 °C[40]), the gold nanoparticles melted while heating at 310 °C for 24 h, and hollow gold spheres were not formed (data not shown). However, for PS−$(PAH/PSS)_4/Au_{NP}$/PEI/PSS particles electroless-plated with a thicker gold layer (∼50 nm), macroporous hollow gold spheres were prepared after calcination (Figures 2a and b). At higher magnification, fused gold nanoparticles were observed (Figure 2b). On the other hand, THF treatment of the PS particles coated with $(PAH/PSS)_4/Au_{NP}$/PEI/PSS, followed by THF and water washing, yielded hollow Au_{NP}/PE spheres (Figures 2c). The hollow spheres made from the nonplated colloids show some change in shape (compared with original template) due to drying of the samples, leading to folding and collapse. Some of the hollow spheres also appear broken, probably due to ultrasound treatment and mechanical forces during washing and sample preparation for TEM. The hollow spheres made from the particles PS−$(PAH/PSS)_2/Au_{NP}$/PEI/PSS after electroless gold plating remain more intact (Figure 2d).

(b) Optical Properties. The particle−particle interactions between the gold nanoparticles for the different systems are reflected in the optical spectra shown in Figure 3. The initial DMAP-stabilized gold sol has a plasmon resonance peak at 517 nm. After formation of composite layers on the PS particles, the peak shifted to 655 nm (for PS−$(PAH/PSS)_2/Au_{NP}$/(PEI/PSS) particles dispersed in water) because of enhanced interactions between the gold nanoparticles[41] and changes in the dielectric medium surrounding the gold nanoparticles.[42] Electroless plating before PS core removal leads to peak broadening (strong extinction from 500 to 850 nm),

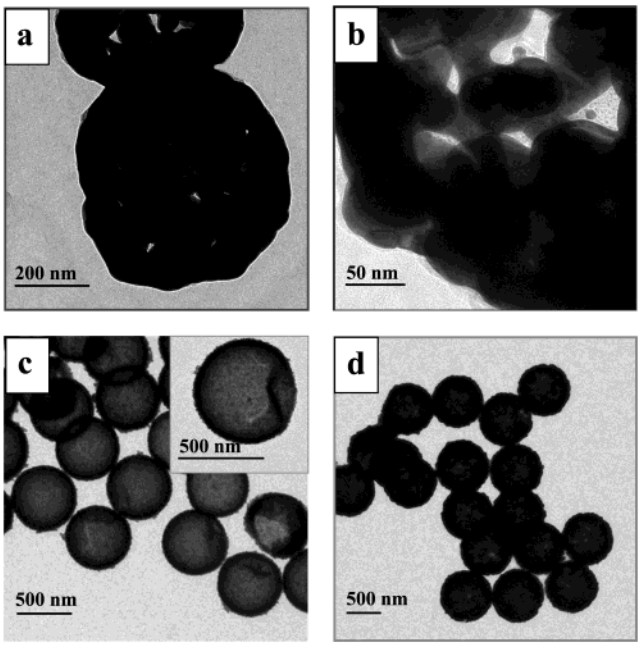

Figure 2. TEM images of PS−$(PAH/PSS)_4/Au_{NP}$/(PEI/PSS) after electroless gold plating, PEI/PSS deposition, and core removal by calcination (a, b), PS−$(PAH/PSS)_4/Au_{NP}$/(PEI/PSS) after core dissolution by THF (no electroless plating) (c), and PS−$(PAH/PSS)_2/Au_{NP}$/(PEI/PSS) after electroless gold plating, PEI/PSS deposition, and dissolution of the core by THF (d).

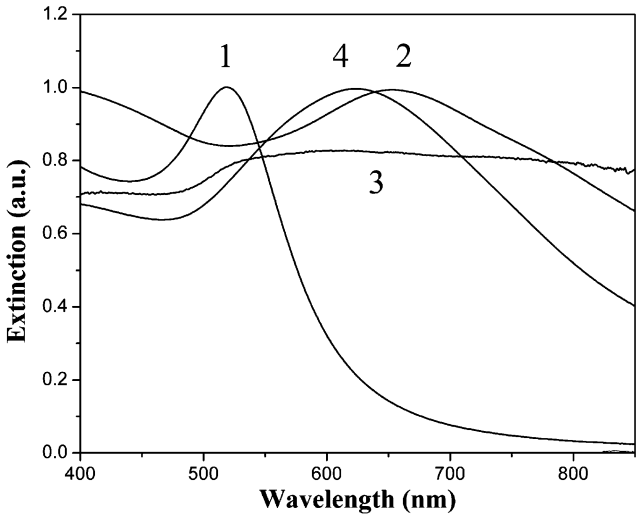

Figure 3. UV−visible extinction spectra of a DMAP-stabilized gold sol (1), and of PS−$(PAH/PSS)_2/Au_{NP}$/(PEI/PSS) core−shell particles before (2) and after (4) PS core removal, and the same core−shell particles after electroless plating (3).

which suggests coalescence of the gold nanoparticles and an increase in thickness of the metal coating on the PS colloids.[22a,31] PS core removal by THF also affects the peak position—a blue shift is observed relative to the core−shell $(PAH/PSS)_2/Au_{NP}$/(PEI/PSS) particles (625 vs 655 nm). This may be explained by a combination of effects: a decrease in the average refractive index and the light scattered by the composite particles, and swelling of the individual hollow spheres in solution.[43]

Increasing the number of preassembled PE layers on the PS colloids affects not only the degree of gold

(40) *Handbook of Chemistry and Physics*, 80th ed.; Lide, D. R., Ed.; CRC Press: Boca Raton, FL, 1999; pp 4−127.
(41) Krebig, U.; Vorde, M. *Optical Properties of Metal Clusters*; Springer-Verlag: Berlin, 1995; Vol. 25.
(42) Leatherdale, C. A.; Bawendi, M. G. *Phys. Rev. B* **2001**, 63, 165315.
(43) Radtchenko, I. L.; Sukhorukov, G. B.; Leporatti, S.; Leporatti, S.; Khomutov, G. B.; Donath, E.; Moehwald, H. *J. Colloid Interface Sci.* **2000**, *230*, 272.

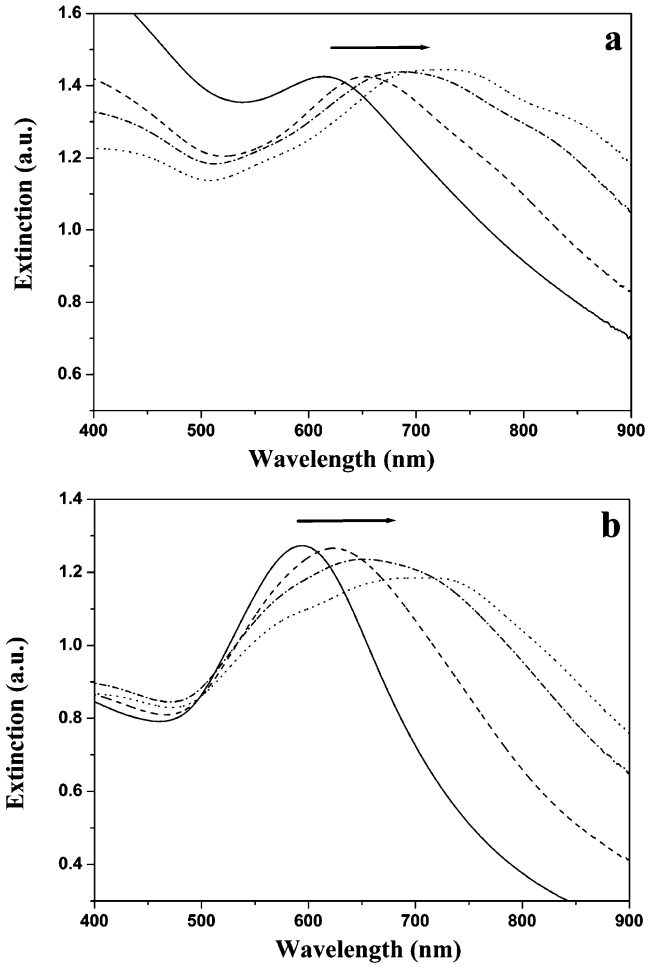

Figure 4. UV−visible extinction spectra of PS−(PAH/PSS)$_x$/Au$_{NP}$/(PEI/PSS) particles (a) and the corresponding hollow spheres obtained after dissolution of the PS core with THF (b) for different PE coating thicknesses: $x = 1$ (solid spectrum), 2 (dashed spectrum), 3 (dash-dotted spectrum), and 4 (dotted spectrum).

nanoparticle loading and the composite particle diameter but also the optical properties of the colloids (Figure 4a,b). The extinction spectra of core−shell PS−(PAH/PSS)$_x$/Au$_{NP}$/(PEI/PSS) ($x = 1, 2, 3, 4$) particles (Figure 4a), and hollow spheres derived from these particles by THF treatment (Figure 4b), show an evident red shift and broadening of the plasmon resonance bands with an increase in PE layer number (i.e., coating thickness). For the core−shell particles, the peak systematically shifted from 615 to 730 nm with increasing polyelectrolyte bilayer number from 1 to 4 and from 595 to 720 nm for the corresponding hollow spheres. The red shift in the spectra could be due to the combined effect of a change in the dielectric constant[42] and coupling of the plasmon resonances in neighboring metal nanoparticles.[41] Increasing of the gold nanoparticle loading in our case will lead to increasing gold particle−particle interactions, thus causing a red shift in the optical spectra. To confirm that the red shift measured was not an artifact caused by scattering, we also used an integrating sphere to measure the diffuse reflectance spectra. Diffuse reflectance spectra of core−shell particles and hollow spheres in solution (data not shown) revealed similar trends to those recorded in the normal absorption mode (that is, a red shift of the extinction peak with an increase in the PE layer number and a blue shift in the spectra of hollow spheres relative to those of the core−shell particles), although the red shifts were less pronounced (50-nm shift from the 1 to 4 bilayer system for the core−shell particles and a 90-nm shift for the corresponding hollow spheres). Similar trends for absorption and diffuse reflectance spectra were recently reported for semiconductor nanoparticles in solution and in solid state.[44]

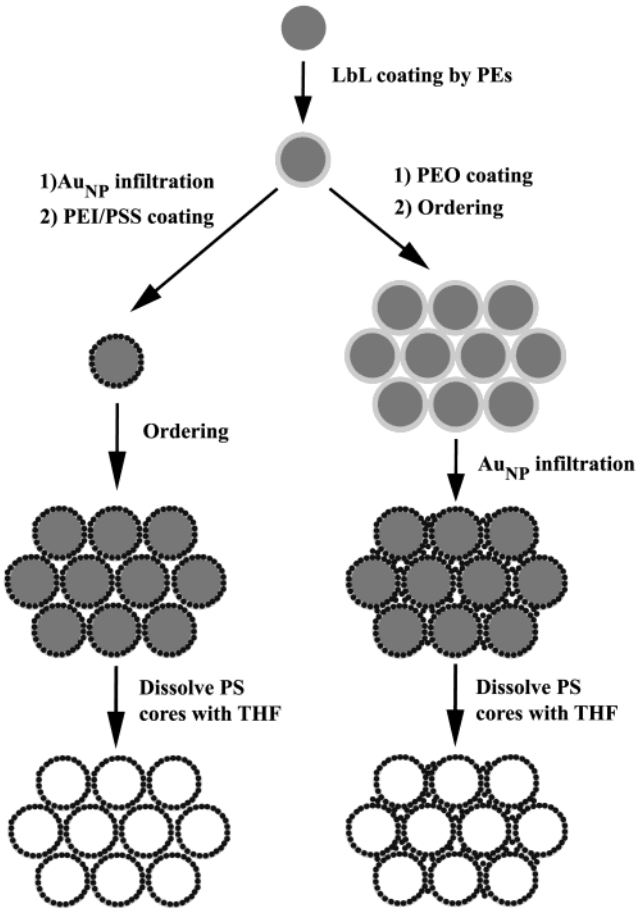

Figure 5. Schematic illustration of the preparation of the core−shell particles and ordered assemblies of the core−shell and hollow spheres.

B. Ordered Assemblies of Core−Shell Particles and Hollow Spheres. *(a) Preparation and Characterization.* Earlier, we demonstrated the ability to form 3D metallodielectric opals using PS−PE$_x$/Au$_{NP}$ core−shell particles.[36] Here, we have produced ordered assemblies of Au$_{NP}$-based *hollow* microspheres. Two different approaches were used (Figure 5). In the first strategy (left part of Figure 5), both 3D ordered arrays made of the PE$_x$/Au$_{NP}$-coated PS spheres (as well as of electroless-plated PE$_x$/Au$_{NP}$-coated PS spheres) were formed by gravity sedimentation of the particles in a circular-cell chamber on hydrophilic quartz substrates. In the second approach (right part of Figure 5), ordered arrays of brushlike PEO-modified PAH/PSS-coated PS spheres were first formed and subsequently exposed to a dispersion of the gold nanoparticles. The use of a PEO outermost layer provided additional stability for the ordered particle template for the Au$_{NP}$ infiltration step.[36]

(44) Dollefeld, H.; Weller, H.; Eychmuller, A. *J. Phys. Chem. B* **2002**, *106*, 5604.

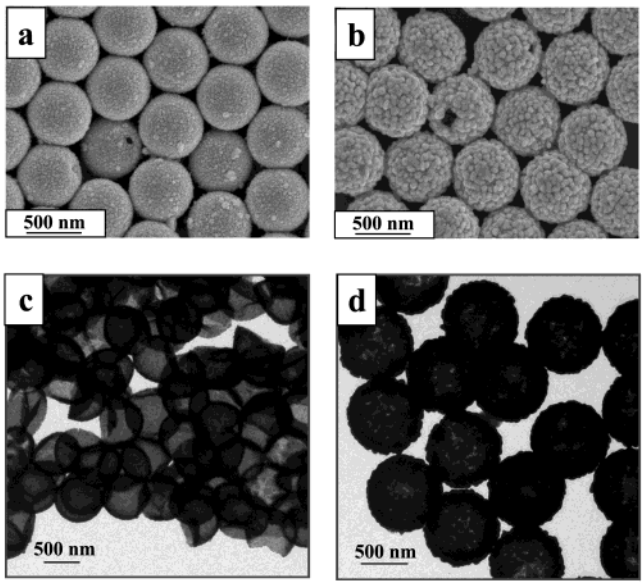

Figure 6. SEM images (a, b) of the ordered assemblies of hollow spheres and TEM images (c, d) of separated hollow spheres prepared by ultrasound treatment of the samples shown in a and b. The ordered assemblies of the hollow spheres (a) were prepared by THF treatment of the ordered assemblies of $(PAH/PSS)_4/Au_{NP}$/PEI/PSS-coated PS spheres (the coated particles shown in Figure 1b) (see left part of Figure 5). Then sonication was used to re-disperse assemblies to obtain separated hollow spheres (c). For (b, d), the $(PDADMAC/PSS)_2/Au_{NP}$-coated PS spheres were electroless gold-plated and then coated with PEI/PSS (the core−shell particles shown in Figure 1(d)), crystallized, and treated with THF (b), followed by sonication (d). The core−shell particles were crystallized by gravity sedimentation and water evaporation.

Additionally, the gold nanoparticles that were infiltrated into the ordered arrays can also serve as seeds for subsequent shell growth using electroless gold plating, resulting in increased gold coverage. For all cases, ordered arrays with different gold content, depending on the number of preassembled PE layers onto the PS spheres, were prepared. Hollow sphere ordered arrays were obtained by exposing the aforementioned ordered arrays of core−shell particles to THF to dissolve the PS cores.

Figure 6a shows an SEM image of an ordered assembly of the hollow spheres made of $(PAH/PSS)_4/Au_{NP}$/PEI/PSS-coated PS spheres after dissolution of the PS cores. TEM images of separated microspheres from the ordered assemblies after ultrasound treatment confirmed dissolution of the cores (Figure 6c). The SEM images of ordered assemblies of PE_x/Au_{NP}-coated PS particles before THF treatment have been reported in our earlier work.[36] Figure 6 may be compared with TEM images of the corresponding separated core−shell and hollow spheres shown in Figures 1 and 2. The center-to-center distances of the $PS-(PAH/PSS)_4/Au_{NP}/(PEI/PSS)$ particles in the ordered assemblies, according to SEM, are 705 ± 5 nm[36] and 660 ± 5 nm (Figure 6a) before and after dissolution of the core, respectively. The core removal step causes a shrinkage of 6%. The shell thickness is 25 ± 5 nm, as measured from the broken spheres (SEM image not shown). Figure 6b shows an SEM image of the assemblies prepared from $(PDADMAC/PSS)_2/Au_{NP}$/PEI/PSS-coated PS spheres that were electroless-plated and additionally coated with PEI/PSS,

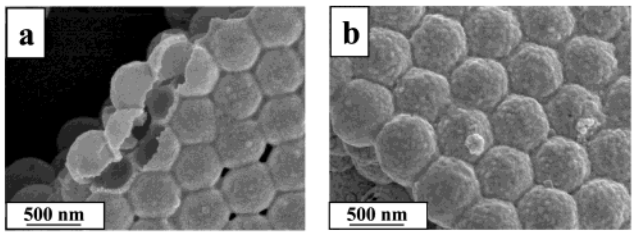

Figure 7. SEM images of ordered assemblies of hollow spheres prepared by Au_{NP} infiltration of ordered arrays of PE_8/PEO-coated PS spheres, followed by dissolution of the PS cores with THF (a) (see right part of Figure 5), or followed by electroless gold plating first and then PS core dissolution (b).

followed by dissolution of the PS cores. Prior to core dissolution, the diameter of the $PS-(PDADMAC/PSS)_2/Au_{NP}$/PEI/PSS spheres after electroless plating is 745 ± 5 nm (from TEM). After core removal, the diameter decreases to 730 ± 5 nm (Figure 6d). The center-to-center distances by SEM are 760 ± 5 and 740 ± 5 nm, respectively, before and after dissolution of the PS cores. A shrinkage of ∼3% occurs as a result of core removal. The shell thickness is 50 ± 5 nm, determined from deliberately broken spheres (SEM image not shown). TEM images after ultrasound treatment of the ordered assembly (Figure 6d) show that the hollow spheres retain their original morphology when they are electroless-plated prior to core dissolution.

Preparation of the gold-containing samples by Au_{NP} infiltration into 3D-ordered assemblies of PE_x/PEO-coated PS spheres has been described elsewhere.[36] In this case, gold nanoparticles infiltrated into both the interstices of the ordered arrays and the PE multilayer coatings on the PS spheres. The gold content, according to TGA data, was 49 wt % ($PS-PE_4/PEO/Au_{NP}$) and 59 wt % ($PS-PE_8/PEO/Au_{NP}$).[36] Figure 7a shows an SEM image of ordered assemblies of hollow spheres prepared from PE_8/PEO-coated PS spheres infiltrated with the Au_{NP} after dissolution of the PS cores. The samples have hexagonal ordered packing with the (111) face parallel to the quartz substrate. SEM observation of the cleaved edges of the samples revealed 3D order. The ordered hollow sphere assemblies ($PE_8/PEO/Au_{NP}$) show a shrinkage of 7% as a result of core removal. The shell thickness, determined from broken spheres, is 28 ± 5 nm. It is noted that the extent of order of the hollow sphere arrays made of $PS-PE_x/PEO/Au_{NP}$ (i.e., infiltration samples) is higher than that observed for the arrays made of $PS-PE/Au_{NP}$/PEI/PSS particles by crystallization of individual composite particles, followed by core dissolution. This may be explained by the fact that the Au_{NP}/PE-coated PS spheres are heavier and have higher surface roughness than the PE_x/PEO-coated PS particles, thus making them more difficult to crystallize. Figure 7b shows an SEM image of the hollow sphere ordered array prepared from PE_8/PEO-coated PS spheres infiltrated with the gold nanoparticles, followed by electroless gold plating and PS core removal. A shrinkage of 4% in the particle diameters as a result of PS core removal was observed. A shrinkage of 15−20% is typically observed for hollow spheres made from core−shell particles by calcination.[35] In the present work, the ordered assemblies of hollow spheres prepared by THF treatment show shrinkages of less than 10%. This may be attributed to the remaining PE in the sphere walls.

After electroless plating, the ordered assemblies show little shrinkage upon dissolution of the cores due to the thicker gold coatings. The stability of the microspheres also depends on the number of preassembled PE_x layers. For $x = 2$ and $x = 4$, SEM revealed the presence of collapsed hollow spheres (images not shown), which may be due to the shell thickness being too thin to form a stable structure.

(b) Optical Properties. Extinction spectra of quartz-supported ordered arrays made of PE_x/PEO-coated PS spheres infiltrated with gold nanoparticles show a gold plasmon resonance peak that is red-shifted relative to that of the gold nanoparticles in solution: The plasmon peak occurred at 517 nm for the Au_{NP} sol. For ordered films of particles, it occurred at 576 nm for PS−PE_2/PEO/Au_{NP}, 583 nm for PS−PE_4/PEO/Au_{NP}, 588 nm for PS−PE_6/PEO/Au, and 603 nm for PS−PE_8/PEO/Au_{NP}. This red shift is due to the coupling of the surface plasmons in neighboring particles (similar to the individual PE_x/Au_{NP}-coated PS particles in solution (Figure 4a)). After electroless gold plating the plasmon resonance showed no measurable peak in the visible range, which may indicate coalescence of the gold nanoparticles and an increase in thickness of the metal coating on the PS colloids, or even the formation of a continuous metal film.[22,41] The spectra of the ordered arrays after dissolution of the PS cores also do not show sharp plasmon resonance peaks characteristic of gold nanoparticles. The increasing absorption of gold at higher wavelengths and broadening of the peak (relative to the ordered arrays before dissolution of the core) may be explained by increasing nanoparticle interactions due to shrinkage after PS core removal. However, the UV−visible extinction spectra of the corresponding separated hollow spheres in solution show a blue-shift relative to the core−shell particles, most probably due to swelling of individual hollow spheres in solution, and hence a decrease of the average refractive index of the composite spheres formed (Figure 3).

The ordered arrays of core−shell particles we have used to prepare the hollow sphere assemblies have a 3D ordered structure. It is well-known that monodisperse colloid spheres of silica or polystyrene spontaneously self-organize into crystal structures at optical wavelength scales with long-range periodicity and possess an optical stop band in the visible to near-IR-spectral ranges depending on the particle diameter.[45] Near-IR reflectance spectra show Bragg reflectance of ordered arrays of PS core particles coated by a Au_{NP}/PE shell.[36] Optical properties of such materials can be controllably modulated through variation of the PE shell thickness of the coated colloids.[36] The near-IR reflectance spectra of the 3D ordered assemblies made of hollow PE_6/PEO/Au_{NP} spheres were measured (curve 2, Figure 8). We examined the near-IR reflectance properties of the hollow sphere arrays made of PS−PE_x/PEO/Au_{NP} (i.e., infiltration samples) only because, as mentioned earlier, the degree of order in these systems is higher than that observed for the crystallized arrays made of PS−PE/Au_{NP}/PEI/PSS particles followed by the core dissolution. The peak position is near 1200 nm, while it is at 1360 nm for colloidal crystals of pure 640-nm-diameter PS[36] and at 1640 nm for the sample with the same composition before the PS core removal (curve 1, Figure 8). The blue shift may be explained by fact that the PS cores have been dissolved and hence the refractive index properties of the system have changed. Shrinkage also leads to a lower wavelength of the peak position. The peak broadening and decrease in intensity may be attributed to a decrease in structural order in the system and by the decrease in refractive index contrast.

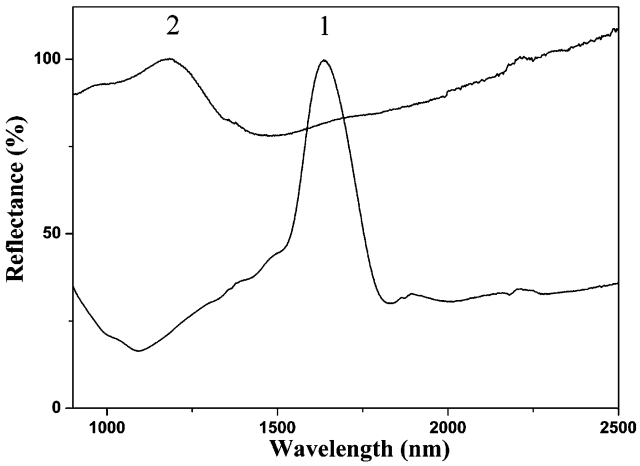

Figure 8. Near-IR reflection spectra of PS−$(PAH/PSS)_3$/PEO/Au_{NP} ordered arrays before (1) and after (2) PS core removal. The angle of incidence is 20°.

Conclusions

We have prepared core−shell particles by the layer-by-layer technique, utilizing PE multilayers assembled onto PS cores as thin films in which to infiltrate gold nanoparticles. The layer thickness of the gold coating was varied from 10 to 50 nm by changing the number of preassembled PE layers used or by additional electroless gold plating of the gold nanoparticle infiltrated layers coated on the PS particles. Hollow spheres were obtained from these particles upon removal of the templated PS cores. UV−visible extinction spectra showed that the plasmon resonance peaks of the Au_{NP} in the core−shell particles and hollow spheres are in the range 595−730 nm, depending on the gold-coating thickness and if the particles were electroless-plated. Thicker gold coatings resulted in a larger red shift in the peak plasmon resonance band. The extinction peak of the hollow Au_{NP}/PE spheres red-shifted relative to that of gold nanoparticles in solution. It also red-shifted for the hollow spheres that had increasing PE layer numbers, but blue-shifted relative to core−shell particles with the same layer composition. The shift in the plasmon peak positions was attributed to changes in the average refractive index of the composites formed and nanoparticle interactions in the layered structures. The core−shell particles, either with PE/PEO or Au_{NP}/PE (with or without electroless plating) coatings, were organized into 3D ordered assemblies. For the PS−PE_x/PEO particles ($x = 2-8$), subsequent Au_{NP} infiltration or electroless gold plating was performed. For the 3D-ordered core−shell particle assemblies, removal of the PS cores led to ordered assemblies of hollow spheres. The UV−visible extinction spectra of the 3D ordered

(45) See, for example, the special issue *Adv. Mater.* **2001**, *13*, 369.

hollow assemblies show a similar trend to that observed for hollow spheres in solution, except for the red shift after removal of the core due to the shrinkage of the structures. From the near-IR reflectance spectra of the 3D ordered hollow assemblies, the Bragg reflectance is blue-shifted relative to the sample before dissolution of the cores.

Acknowledgment. We thank P. Schütz (MPI) and U. Blöck (Hahn-Meitner-Institute) for the TEM measurements and N. Gaponik and D. Talapin (Hamburg University) for help with recording the optical spectra. S. Mayya, T. Cassagneau, and D. Wang (MPI) are thanked for helpful discussions. H. Möhwald is acknowledged for supporting this work within the MPI-Interface department. Funding was provided by the DFG, the Volkswagen Foundation, the BMBF, and the Australian Research Council.

CM031014H